Modern Environmental Science and Engineering (ISSN 2333-2581)
May 2018, Volume 4, No. 5, pp. 469-475
Doi: 10.15341/mese(2333-2581)/05.04.2018/009
Academic Star Publishing Company, 2018
www.academicstar.us

Multi-objective Optimization of a Linear Flexure-Based Mechanism Using Pseudo Rigid-Body Diagram Analysis and FEA-Based Response Surface Methodology

Khien-Van Nguyen[1,2], Hoang-Huy Pham[3], and Huy-Tuan Pham[1]

1. Faculty of Mechanical Engineering, HCM City University of Technology and Education, Vietnam

2. Vocational and Technical College of Nam Sai Gon, Vietnam

3. Faculty of Mechanical Engineering, HCM City University of Technology, Vietnam

Abstract: This paper presents the optimization design of a linear flexure-based mechanism (LFBM). The design process includes three phases: (1) building a Pseudo Rigid-Body (PRB) model for the mechanism (2) converting the PRB diagram into a compliant mechanism (CM) model, and (3) optimizing the CM model using the Response Surface Methodology. In the design of the LFBM, circular flexure hinges are used to provide accurate linear movement and large displacement. The circular flexure hinges are combined with rigid links to synthesize lever mechanisms and parallelogram mechanisms to gain large magnification, increase rigidity and decrease parasitic motion. The PRB diagram analysis method and surface response methodology based on finite element analysis (FEA) are used to solve the multi-objective optimization. The objectives of the optimization are to improve the static characteristics as well as the dynamics of the linear motion mechanism. FEA-based experiments are conducted to evaluate the validity of the model. The analysis and simulation results show that the operational range of the LFBM is larger than 200 μm, and the first-order natural frequency is above 350 Hz.

Key words: flexure mechanism, pseudo rigid-body diagram, response surface methodology, ANOVA

1. Introduction

Compliant mechanism (CM) has been receiving a significant consideration due to its huge potential application in precision engineering. It can be used to design ultra-precision positioning devices such as fast tool servo for turning manufacturing [1, 2]; 2-DOF positioning platform [3]; nanoprecision 3-DOF vertical positioning system [4]; microgripper for high precision micro-object manipulation [5]; constant-force mechanism for force regulation [6-7]; storage case for disk-shaped media [8]; bistable relay [9]. The noteworthy usage of CM compared to kinematics mechanisms are due to its numerous advantages: compactness; reduced wear, noise, vibration and need for lubrication; light weight, increased precision since backlash is eliminated, therefore ease of miniaturization [10].

Theoretically, there are three groups of synthesis approaches for CM: (1) the kinematics based approaches, (2) the building blocks approaches and (3) the structural optimization based approaches including topology and shape optimization. In the last group, commonly used methods consist of Genetic Algorithm (GA) [11-12], hybrid Taguchi-differential evolution algorithm [13], Gene Algorithm and Taguchi–based sensitivity analysis [14], and Response Surface Methodology (RSM) [3].

Compliant mechanisms composed of compliant and stiff elements realizing a desired mobility as the result

Corresponding author: Huy-Tuan Pham, Dr.; research areas/interests: compliant mechanism. E-mail: phtuan@hcmute.edu.vn.

of the elastic deformation of the whole structure rather than because of the relative displacement of the links. In CM, flexure hinges are used to replace for kinetic pairs (i.e., revolute, prismatic, planar, etc.). During the synthesis of CM, some researches only focus on the design of flexure hinges (minimum thickness, shape and size of the notch) without taking into consideration of the kinematic dimensions of the links. Although flexure hinges play a crucial role in realizing the deformation of the CM [15-16], kinematic dimensions of the rigid links significantly affect the displacement, parasitic motion, and magnification of the structures [10]. In order to take into consideration for these factors simultaneously without turning the design task cumbersome, this paper proposes a new synthesis approach in 2 steps which (1) analyses the dimensions of rigid links by using Pseudo Rigid-Body (PRB) diagram and (2) optimizes the size of flexure hinges with FEA-based RSM. Finally, a multi-objective optimization is implemented to enhance the static and dynamic characteristics of the linear compliant guide mechanism for high precision manufacturing processes.

In order to enhance the synthesis procedure of the CM in this research, PRB diagram analysis is undertaken by establishing the kinematic relation for the links. A mathematical model is built by analytical method. Gradient-based optimization is then applied to find the optimum link dimensions. These dimensions will be set as constant for the next step to reduce the number of design parameters. Due to the approximation assumption made in the preliminary mathematical model, a more accurate method should be applied to eliminate those errors. Next, FEA-based RSM is implemented in the following procedure: (i) first, 3D model of the structure is built using ADPL codes in ANYS; (ii) assign independent variables as input parameters; (iii) define response surfaces as outputs; (iv) determine the effect of input parameters to the responses and formulate the mathematical models, and (v) finally, solve for the optimum design variables (DVs) and responses.

The pros of the proposed synthesis method of CM in this research compared to the other methods are:

(1) Key DVs of the device are determined by PRB model. Then RSM is used to analyse the static, kinematic and dynamic behaviours of the structure. Finally multi-objective optimization is used to optimize the displacement and natural frequency.

(2) Design of experiments setting up in ANSYS make it very simple and straightforward.

(3) FEA-based RSM helps to build the objective functions related to DVs. These mathematical functions could direct to the global optimum.

2. Design

2.1 Working Principle

A linear flexure-based mechanism developed in this paper can be used for a feed drive mechanism in ultra-precision turning manufacturing. The concept of the mechanism is the integration of two lever mechanisms connected in series to amplify the translation motion from a piezoelectric actuator. This actuator can generate continuous expansion or retraction motion with infinite resolution, zero backlash, and wide dynamic response range. Between the levers and the machining tool, two parallelogram flexure mechanisms are incorporated to enhance the stiffness and minimize the parasitic motion. The schematic diagram of this mechanism is illustrated in Fig. 1.

The working principle of the feed drive mechanism is illustrated in Fig. 1. Ultra-precision linear motion is driven by the PZT actuator, the CM, a screw and a fixture. The PZT actuator is connected to the CM via a screw which can provide a preload. The linear mechanism is designed to have the output motion axial to the translation input of the actuator. These motions are in the same direction to prevent the shear stress and torsion applied to the PZT actuator. To drive the mechanism, an electrical voltage should be applied to the PZT actuator which will induce expansion. It will

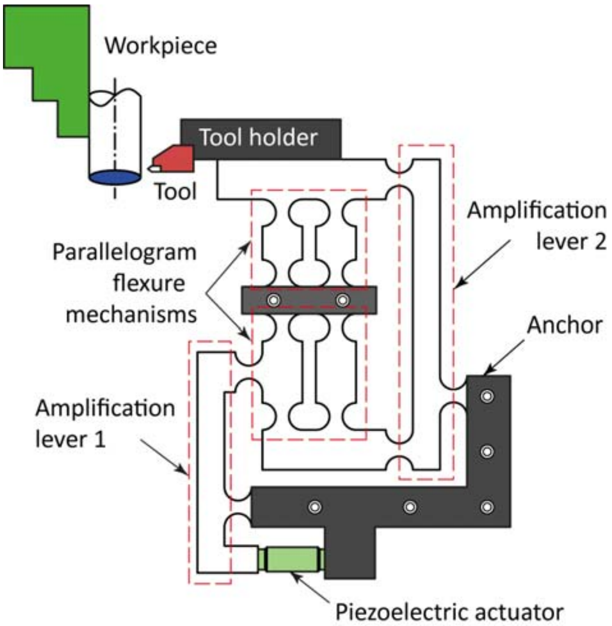

Fig. 1 Schematic diagram of the high precision feed drive mechanism.

push the lever mechanism 1. Via the parallelogram mechanism, this displacement will be transmitted to the lever mechanism 2 and finally, the cutting tool will be fed to the workpiece. When the position of the tool has been fixed, a gripping mechanism (mechanical or solenoid) will be activated to hold it. After the manufacturing process finishes, the gripping mechanism is detached, electrical power is turned off, PZT and tool return to their initial states.

2.2 Problem Formulation

2.2.1 Amplification Analysis (in x Direction)

In Fig. 2(a), let x_p, x_1, x_2, x_{out} be the displacement of the PZT actuator, the lever mechanism 1, the parallelogram mechanism 1, and the lever mechanism 2, respectively. The amplification ratio of the feed drive mechanism can be calculated as:

$$A_{amp} = \frac{x_{out}}{x_p} = \frac{L_2(L_4 + L_3)L_6}{L_1 L_4 L_5} \quad (1)$$

2.2.2 Analysis of Parasitic Motion (y Direction)

The displacement in y direction of the mechanism largely affects the precision of the feeding movement (in x direction). It must be carefully calculated and

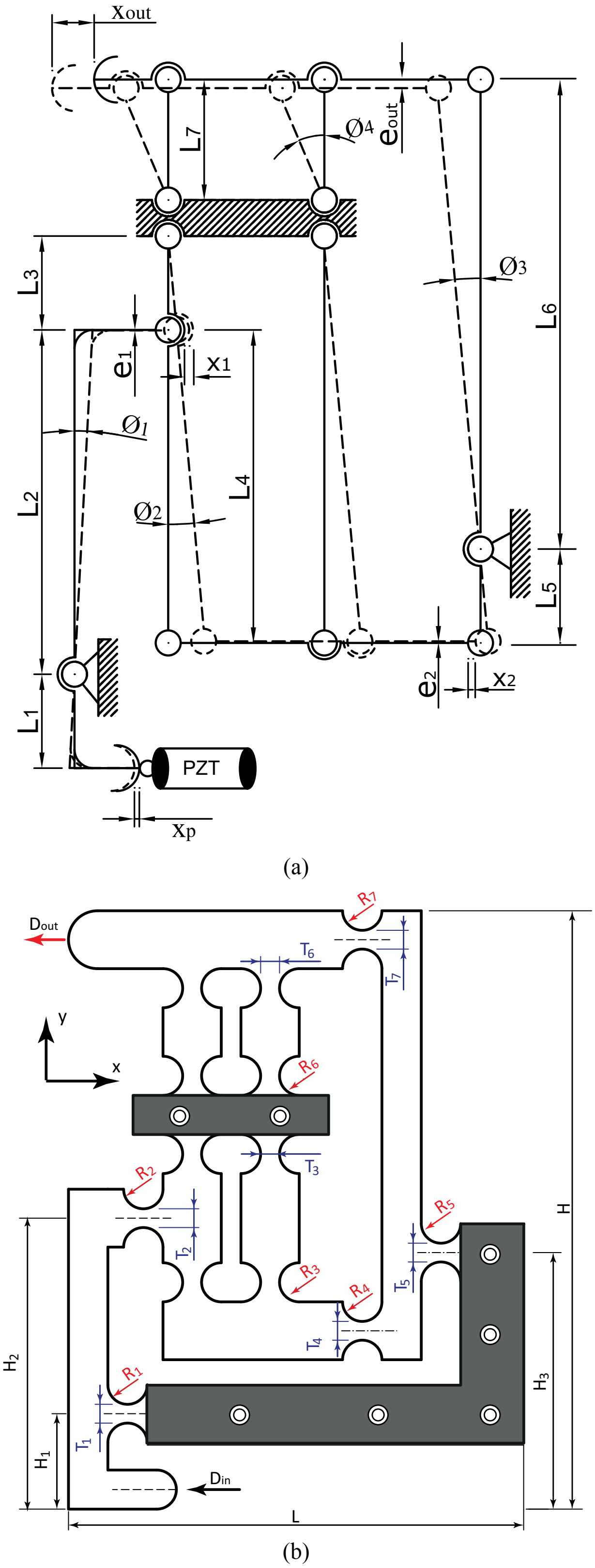

Fig. 2 Kinematic diagram of the PRB model (a) and its compliant counterpart (b).

constrained during the operation. Let e_1, e_2, e_{out}, be the parasitic motion of the lever 1, the parallelogram and lever 2, respectively (Fig. 2a). These displacements are calculated as following:

$$e_1 = L_2 - \sqrt{L_2^2 - x_1^2} \tag{2}$$

$$e_{out} = L_7 - \sqrt{L_7^2 - x_{out}^2} \tag{3}$$

$$e_{out} = L_7 - \sqrt{L_7^2 - \left(\frac{x_p L_2 (L_4 + L_3) L_6}{L_1 L_4 L_5}\right)^2} \tag{4}$$

The PRB model in Fig. 2(a) can be converted to the CM whose shape is presented in Fig. 2(b). During the conversion, revolute joints can be replaced by flexure hinges with different shapes (circular, ellipse, parabolic, hyperbolic) [15-16]. In this research, semi-circular hinge is used due to its advantages: lower stress concentration, simple and easy to fabricate [17]. Aluminium 7075-T6 is chosen for this linear flexure mechanism due to its high yield strength to Young's modulus ratio. Its Young's modulus (E), yield strength (σ_y), Poisson rate (υ) and density (ρ) are 71.7 GPa, 500 MPa, 0.33, and 2810 kg/m^3, respectively. This device can be fabricated by wire electrical discharge machining (WEDM).

3. Optimization

3.1 PRB Model Optimization

Since the displacement amplification of the PRB diagram is one of the objective functions of the design, and it has been formulated in Eq. (1). This function can be optimized by using MATLAB with "*fmincon*" and the expected amplification ratio of the mechanism is 5. All DVs are shown in Fig. 2(a), design constraints, boundary conditions and objective function are formulated in Table 1.

3.2 Compliant Mechanism Optimization

The overall dimension of the linear feed drive mechanism is fixed at (90x150x8) mm. These dimensions have been carefully considered to ensure for the assembly to the CNC turning machine. Considering the DVs, according to the theory of CM [10], the maximum stress of flexure hinges highly depends on the minimum thickness of the notch (t) and is described by the following equation:

$$\sigma_{max} = \frac{6 M_z K_t}{t^2 b} \tag{5}$$

where σ_{max}, M_z, K_t, t, b are maximum stress, bending moment along z axis, stress concentration factor, minimum thickness and width of flexure hinges.

In order to confirm for the processing possibilities and practical realization of the feed drive mechanism, it is expected to create large displacement in the x direction and possess high natural frequency. The later requirement can enhance the operation speed of the system. Therefore, 2 objective functions are chosen for the problem. y_1 and y_2 are the displacement along x axis and first natural frequency, respectively. Design variables are shown in Fig. 2(b). The multi-objective optimization flowchart is presented in Fig. 3. Design constraints, boundary conditions and objective functions are formulated in Table 3.

Table 1 Formulation of the PRB model optimization.

1. Objective: $\min \left| A_{amp} - 5 \right|$	(6)
2. Design variables: $L_1 \div L_6$	
3. Constraints:	
(i) Inequality constraints:	
$15 \le L_1 \le 25$	(7)
$20 \le L_4 \le 40$	(8)
$15 \le L_5 \le 25$	(9)
(ii) Equality constraints :	
Design space: L*H	
L = 150 (mm); H = 90 (mm)	
$L_1 + L_2 = 70$	(10)
$L_3 + L_4 = 60$	(11)
$L_5 + L_6 = 90$	(12)
(iii) Parasitic motion constraint:	
$e_{out} \le 7\mu m$	(13)

Table 2 Value of the optimum variables.

DVs	Value (mm)	DVs	Value (mm)
L_1	20	L_4	30
L_2	50	L_5	20
L_3	30	L_6	70

Table 3 Formulation of multi-objective optimization of the CM.

1. Objective :	
$Max[y_1(T_1, T_2, T_3, T_5, T_6)] \geq 150\mu m$	(14)
$Max[y_2(T_1, T_2, T_3, T_5, T_6)] \geq 300Hz$	(15)
2. Design variables : $T_1 \div T_3$, T_5, T_6	
3. Constraints :	
(i) Design variables (mm)	
$1.5 \leq T_1 \leq 2.7$	(16)
$1.0 \leq T_2, T_3 \leq 1.7$	(17)
$0.3 \leq T_5, T_6 \leq 0.7$	(18)
(ii) Parasitic motion: $u_y \leq 7\mu m$	(19)
(iii) Maximum stress: $\sigma_m \leq \frac{\sigma_y}{SF}$	(20)

Fig. 3 Flowchart of the multi-objective optimization for the linear flexure mechanism.

4. Results and Discussions

4.1 FEA-based RSM

In RSM, according to the amount of DVs, the number of design of experiments (DoEs) can be determined by using the CCD method. The number of required DoEs is determined by [18]:

$$N = 2^{k-f} + 2k + n_c \tag{21}$$

where N, k, f, n_c are the total number of experiments, number of DVs, factorial number, and number of replicates at the center point of the design space, respectively.

In this design, k = 5 and f = 1. In order to do the analysis, only 1 experiment is necessary at the center of design space, therefore n_c = 1. From Eq. (21), there are 27 design points are required for the DoE. These 27 design points are automatically generated in ANSYS 15. They are then analysed by Minitab 16.0. The resulted regression equations for the 2 responses (y_1, y_2) in relation to the 5 DVs are:

$$y_1 = 0.159 + 0.005T_1 - 0.005T_2 - 0.003T_3 - 0.014T_5 - 0.019T_6 + 0.007T_3^2 \tag{22}$$

$$y_2 = 444 + 3.375T_2 + 3.130T_3 + 19.273T_5 + 23.879T_6 + 4.158T_5^2 - 10.187T_3^2 \tag{23}$$

It is suggested that these results should be compared to the Student and Fisher standard to verify the regression model. Table 4 shows the goodness-of-fit of the response surfaces. In statistics, the R^2 value should be above 0.8 for the statistical model to be good. In Table 4, R^2 = 1 and root mean square error (RMSE ≅ 0) approve for the accuracy of the predicted model.

Fig. 4 shows the comparison between the output responses predicted from the developed response surfaces and those obtained at the design points. It can be seen that all data points lie exactly on the straight line. It proves that there is a good agreement for the predicted models by using the FEA-based RSM in ANSYS.

Table 4 The goodness-of-fit of the response surfaces.

Parameters	y_1	y_2
R^2	1	1
MRR	0	0
RMSE	9.24×10^{-11}	1.08×10^{-7}
RRMSE	0	0
RMAE	0	0
RAAE	0	0

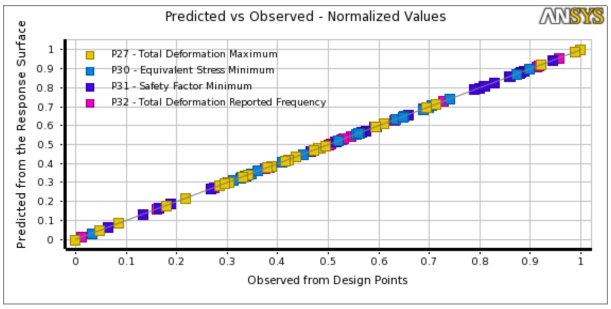

Fig. 4 Comparison between the response surfaces and design points.

Analysis of variance (ANOVA), F-value and p-value test [20] are conducted to check the sufficiency of the developed mathematical models of y_1 and y_2. The results of ANOVA in Table 5 shows a very good F-value of both models since they are all higher than the critical value of F-distribution of 2.59 from the standard table at 95% confidence level. P-value is used to verify for the significant of model terms, and this value should be less than 0.05. Table 5 also shows that both models have this value smaller than 0.001. The ANOVA results confirm that the developed models for y_1 and y_2 are sufficient and accurate.

4.2 Optimum Results

After running through all optimization processes, three candidates are found in Table 6. Among them, candidate 1 is chosen as the best design due to its highest displacement. Its 1st natural frequency is also higher than requirement ($f_0 = 388.5$ Hz)

In comparison to the initial design, the optimal design has better static and dynamic behaviours which are shown in Table 7. The deformation shape of the optimum design is shown in Fig. 5 and its first natural frequency is shown in Fig. 6.

Table 5 Results of ANOVA

Models	Source	F-value	p-value	Remarks
y_1	Regression	40.30	0.000	Significant
y_2	Regression	48.08	0.000	Significant

Table 6 Comparison among candidates.

DVs	**Candidate 1**	Candidate 2	Candidate 3
T_1 (mm)	***2.70***	2.69	2.67
T_2 (mm)	***0.90***	0.99	0.96
T_3 (mm)	***1.50***	1.73	1.62
T_5 (mm)	***0.30***	0.49	0.31
T_6 (mm)	***0.30***	0.33	0.42
y_1 (mm)	***0.277***	0.186	0.192
y_2 (Hz)	***388.5***	421.3	412.2

Table 7 Comparison between initial design and optimal design.

Initial design	Optimal design	Improvement (%)
$y_1 = 149$ μm	$y_1 = 277$ μm	85.906
$y_2 = 77.89$ Hz	$y_2 = 388.5$ Hz	389.780

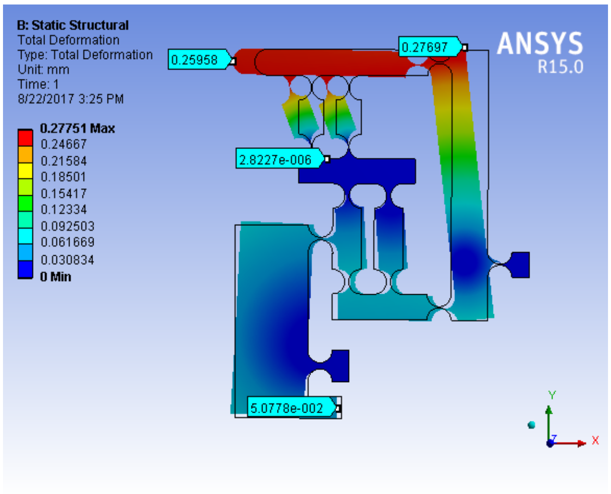

Fig. 5 Deformation of the mechanism.

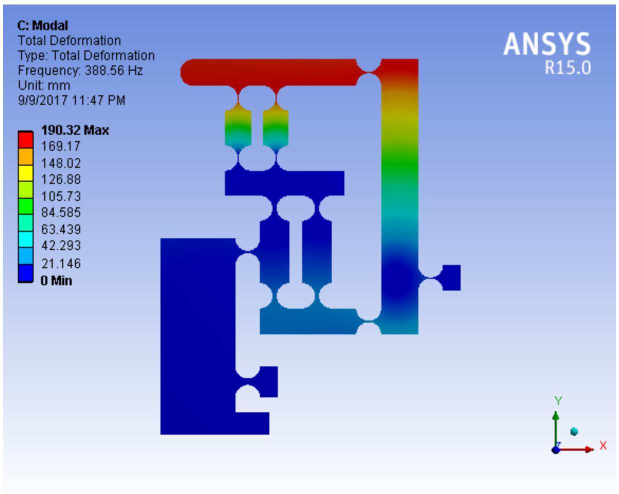

Fig. 6 First natural frequency.

5. Conclusion

This paper has proposed a new multi-objective optimization method for the design of a linear flexure mechanism. In this approach, analysis of a PRB model is done first to screen out significant DVs. Next FEA-based RSM is implemented in ANSYS to find for mathematical models describing the responses of the mechanism. FEA is used to analyse the sensitivity of each DVs to the 2 response surfaces: output displacement along x-axis and natural frequency. The final optimum design has the overall dimensions of (90 mm × 150 mm), output displacement, natural frequency, maximum stress, and safety factor are 277 μm, 388.5 Hz, 171.8 MPa, and 2.92, respectively. This mechanism is going to be fabricated by using WEDM. A controller system should also be designed to control the nonlinear behaviours. It will be installed to the feeding mechanism in a CNC turning machine with accuracy in micrometre or even sub-micrometre.

Acknowledgement

The authors are thankful for the financial support from the HCMC University of Technology and Education, Vietnam, under Grant No. T2018-00NCS.

References

[1] Y. Tian et al., A flexure-based mechanism and control methodology for ultra-precision turning operation, *Precision Engineering* 33 (2009) 160-166.

[2] Q. Liu et al., A flexure-based long-stroke fast tool servo for diamond turning, *Int. J. Adv. Manuf. Technol.* 59 (2012) 859-867.

[3] S. C. Huang and T. P. Dao, Design and computational optimization of a flexure-based XY positioning platform using FEA-based response surface methodology, *International Journal of Precision Engineering and Manufacturing* 17 (2016) (8) 1035-1048.

[4] H. Kim et al., Development of a nanoprecision 3-DOF vertical positioning system with a flexure hinge, *IEEE Trans. Nanotechnol.* 12 (2013) (2) 234-245.

[5] N. M. Z. Mohd et al., Development of a novel flexure-based microgripper for high precision micro-object manipulation, *Sensors and Actuators A* 150 (2009) 257-266.

[6] H. T. Pham and D. A. Wang, A constant-force bistable mechanism for force regulation and overload protection, *Mechanism and Machine Theory* 46 (2011) 899-909.

[7] H. T. Pham and D. A. Wang, A quadristable compliant mechanism with a bistable structure embedded in a surrounding beam structure, *Sensors and Actuators A* 167 (2011) 438-448.

[8] Hilton et al., Storage case for disk-shaped media having a bistable ejection mechanism utilizing compliant device technology, United States Patent, No. 5,590,768 (1997).

[9] J. Qiu et al., A bulk-micromachined bistable relay with u-shaped thermal actuators, *Journal of Microelectromechanical Systems* 14 (2005) 1099-1109.

[10] L. L. Howell, *Compliant Mechanisms*, New York, Wiley, 2001.

[11] J. A. Gallego and J. L. Herder, Synthesis methods in compliant mechanisms: an overview, in: *Proceedings of the ASME 2009 International Design Engineering Technical Conferences & Computers and Information in Engineering Conference (IDETC/CIE 2009)*, San Diego, California, USA, 2009, pp. 1-22.

[12] H. T. Pham, V. K. Nguyen and V. T. Mai, Shape optimization and fabrication of a parametric curved segment prosthetic foot for amputee, *Journal of Science and Technology: Technical Universities* 102 (2014) 89-95.

[13] T. P. Dao et al., Robust parameter design for a compliant microgripper based on hybrid taguchi-differential evolution algorithm, *Microsystem Technologies* (2017) 1-17.

[14] V. K. Nguyen, H. T. Pham and H. H. Pham, Optimal design of flexure mechanism using gene algorithm and taguchi-based sensitivity analysis, in: *International Conference on Systems Science and Engineering*, HCM City, Vietnam, 21-23 July, 2017, pp. 412-417.

[15] N. Lobontiu, *Compliant mechanisms: Design of Flexure Hinges*, CRC Press LLC, 2003.

[16] S. T. Smith, *Flexures Elements of Elastic Mechanisms*, Gordon and Breach Science Publishers, 2000.

[17] G. Chen et al., A tensural displacement amplifier employing elliptic-arc flexure hinges, *Sensors and Actuators A* 247 (2016) 307-315.

[18] ANSYS, Workbench user's guide, available online at: http://148.204.81.206/Ansys/150/Workbench%20Users%20Guide.pdf.

[19] M. Kutner, C. Nachtsheim, J. Neter, and W. Li, *Applied Linear Statistical Models* (5th ed.), McGraw-Hill, 2004, pp. 2-27.

[20] P. J. Ross, *Taguchi Techniques for Quality Engineering*, McGrawHill, 1996, pp. 5-295.